Clays and Clay Minerals, Vol. 64, No. 5, 560–570, 2016.

ADSORPTION OF Cu(II) ON RHAMNOLIPID-LAYERED DOUBLE HYDROXIDE NANOCOMPOSITE

YAN LI[1,*], HAO-YU BI[2], HUI LI[1], AND YONG-SHENG JIN[1]

[1] Department of Chemistry, Changzhi University, Changzhi, 046011, P. R. China
[2] Department of Biomedical Engineering, Changzhi Medical College, Changzhi, 046000, P. R. China

Abstract—A rhamnolipid-layered double hydroxide (RL-LDH) nanocomposite, derived from the rhamnolipid (RL) biosurfactant, was synthesized through a delamination/reassembling process. The adsorption characteristics of Cu(II) on RL-LDH were investigated in detail and the results indicated the potential of using RL-LDH as an environmentally friendly adsorbent to remove Cu(II). The fabricated RL-LDH nanocomposite was characterized using powder X-ray diffraction, Fourier-transform infrared spectroscopy, scanning electron microscopy, transmission electron microscopy, elemental chemical composition, and specific surface area analyses. Batch adsorption experiments were conducted to study the influence of various factors, such as contact time, initial Cu(II) concentration, temperature, initial solution pH, and electrolyte concentration on Cu(II) adsorption by the RL-LDH nanocomposite. The RL-LDH nanocomposite had a low surface area of 11.71 $m^2 g^{-1}$, which suggests that surface adsorption would not be important in Cu(II) adsorption. The Cu(II) adsorption data fitted the Freundlich model well at pH 5.5, whereas the adsorption kinetics were accurately described by a pseudo-second-order kinetics model. Chemical binding, that is, the formation of a RL-Cu(II) complex in the LDH interlayer, was assumed to be the rate-limiting step in the adsorption process. Thermodynamic parameters that included Gibbs free energy, enthalpy, and entropy changes were also calculated. The adsorption was found to be a spontaneous and exothermic chemisorption process. Furthermore, the adsorption properties of RL-LDH for Cu(II) were compared to Cu(II) adsorption using other adsorbents.

Key Words—Adsorption Kinetics, Cu(II), Isotherm, Layered Double Hydroxide, Rhamnolipid.

INTRODUCTION

Heavy metals released into the environment by various household and industrial effluents are major pollutants to plants, animals, and humans. These elements feature high toxicity, non-biodegradability, mobility in natural water ecosystems, and bioaccumulation in living tissues (Awual *et al.*, 2013). Among these heavy metals, Cu(II) is a common contaminant in wastewater. Excessive Cu(II) consumption can cause harmful effects on the liver and the kidneys and can induce anemia, immunotoxicity, and developmental toxicity (Bhattacharyya *et al*., 2011). As such, Cu(II) must be removed from wastewater to protect public health and the environment. Removal can be achieved through chemical precipitation (Matlock *et al*., 2002), adsorption (Bhattacharyya *et al*., 2011), ion exchange (da Fonseca *et al*., 2005), membrane filtration (Venkateswaran 2007), and electrochemical treatment (Mohammadi *et al*., 2005). Adsorption is an attractive choice because of the high efficiency, easy operation, flexible design, no chemical sludge is produced, and the potential recovery of Cu(II) (Sud *et al*., 2008).

Escalating environmental considerations on the use of commercial adsorbents led to the development of available and accessible biological materials as potential metal adsorbents (Inyang *et al*., 2012). In this regard, researchers investigated the ability of biosurfactants to bind to heavy metal ions (Dahrazma and Mulligan, 2007). Studies showed that biosurfactants can be used to treat wastewater contaminated with heavy metals because these compounds exhibit greater environmental compatibility, lower toxicity, and higher biodegradability than synthetic surfactants (Mulligan, 2009).

Rhamnolipid (RL) is a biosurfactant produced by *Pseudomonas aeruginosa* and exists in six structural forms that include R1 monorhamnosyl and R2 dirhamnosyl, which are produced commercially. The RL can form complexes with a wide range of metal contaminants, such as the aqueous cations of Pb, Cd, and Hg because of the RL hydrophilic carboxylate group, which serves as an active reaction site for metal ions (Ochoa-Loza *et al*., 2001); RL can, therefore, be used to remove heavy metals from contaminated soils (Torrens *et al*., 1998).

Layered double hydroxides (LDHs), also known as anionic clays with layered structures, exhibit good adsorption properties and have been increasingly used for the adsorption of anionic contaminants from wastewater. LDHs intercalated with RL (RL-LDH nanocomposites) could be considered as potential heavy metal absorbents due to the strong ability of RL to complex with heavy metals, but the process for separating RL-LDH nanocomposites from wastewater after adsorption

* E-mail address of corresponding author:
liyan_china@126.com
DOI:10.1346/CCMN.2016.064034

is relatively difficult. Recently, magnetic core-shell Fe_3O_4@LDH composites were prepared to effectively remove and quickly separate pollutants from wastewater (Shan *et al*., 2014). As such, magnetite Fe_3O_4@(RL-LDH) nanocomposites, which can be easily separated from aqueous solutions, can be developed and used to act as magnetic adsorbents for Cu(II). Obviously, the premise of realizing the application of Fe_3O_4@(RL-LDH) composites in wastewater treatment is in investigating the adsorption characteristics of RL-LDH nanocomposites. In addition, because the effectiveness and structural typology of LDHs intercalated with RL have been little investigated (Chuang *et al.*, 2010), the synthesis method used to prepare RL-LDH nanocomposites was paid particular attention in this study. In the present work, a delamination/reassembling process was described for the facile fabrication of RL-LDH nanocomposites. The ability of RL-LDH to adsorb Cu(II) was then assessed by studying adsorption kinetics, isotherms, thermodynamics, mechanisms, and by determining the factors that affect the adsorption process.

EXPERIMENTAL METHODS

Materials

Monorhamnosyl RL (>90%) was purchased from Zijin Biological Technology Co., Ltd. (Huzhou, Zhejiang, China). All other reagents were of analytical reagent grade and were used without further purification. These reagents were supplied by Tianjin Chemical Reagent Co. Ltd., Tianjin, China. Double-distilled water (DDW), which was used throughout the study, was boiled for more than 30 min to remove dissolved carbon dioxide.

Modification of Mg-Al-NO_3-LDH with RL

A Mg-Al-NO_3-LDH (LDH) was synthesized through co-precipitation (Qiu and Hou, 2009). The appropriate amounts of $Mg(NO_3)_2{\cdot}6H_2O$ and $Al(NO_3)_3{\cdot}9H_2O$ (the molar Mg^{2+}/Al^{3+} ratio was 3) were dissolved in DDW to obtain a solution with a total metal ion concentration of 0.5 mol L^{-1}. A 0.25 mol L^{-1} NH_4OH solution was slowly poured into the above solution under stirring until a pH of 9.5 was attained. After standing at room temperature for 1 h, the suspension was filtered and the precipitate was peptized at a constant temperature of 80ºC in an oven for ~24 h. Finally, the sample was dried and triturated.

The RL-LDH was prepared by a delamination/reassembling process (Lu *et al*., 2013). Briefly, 0.5 g of LDH was dispersed in 20 mL of formamide under magnetic stirring. The mixture was sonicated to be transparent and then stored overnight at room temperature to yield LDH nanosheets. Subsequently, 20 mL of the LDH nanosheet dispersion was dropped into 20 mL of RL/ethanol solution containing 1 g of RL under slow magnetic stirring and allowed to equilibrate for 30 min. The suspension was centrifuged at 11,125 × g for 15 min, and the supernatant was removed. The precipitate was washed twice with DDW and once with ethanol in a re-dispersion/centrifugation cycle, and the RL-LDH was finally collected and dried in vacuum at 60ºC.

Characterization

Powder X-ray diffraction (PXRD) data were recorded on a Rigaku D/max-γB X-ray diffractometer (Rigaku Corporation, Tokyo, Japan) equipped with CuKα radiation (λ = 0.1542 nm) and scanned from 2º to 80º2θ at 40 kV and 40 mA.

Fourier-transform infrared (FTIR) spectra of the samples were determined using an Avatar 380 spectrometer (Thermo Electron Corporation, Waltham, Massachusetts, USA) at room temperature. FTIR spectra in the 400−4000 cm^{-1} range were collected for samples prepared as KBr disks.

Thermal gravimetry-differential scanning calorimetry (TG-DSC) was performed in an airflow using a STA 449C thermo-gravimetric analyzer (Netzsch-Geratebau GmbH, Selb, Bavaria, Germany) at a heating rate of 10ºC min^{-1}.

A model S4800 scanning electron microscope (SEM, Hitachi, Tokyo, Japan) was used to observe the morphology of LDH and RL-LDH (Liu *et al*., 2013). Additionally, transmission electron microscope (TEM) images of LDH and RL-LDH were recorded on a Tecnai G^2 F20 transmission electron microscope (FEI Company, Hillsboro, Oregon, USA).

Elemental chemical analyses for Mg and Al contents were conducted using a ICAP-9000 inductively coupled plasma atomic emission spectroscope (Thermo Jarrell Ash, Franklin, Massachusetts, USA) by dissolving samples in a dilute HNO_3 solution. Elemental compositions (C, H, and N) of the samples were determined by dry combustion with a Vario EL cube elemental analyzer (Elementar Analysensysteme GmbH, Hanau, Hessen, Germany).

Specific surface areas of the samples were calculated from N_2 adsorption isotherms by the BET method. The samples were outgassed at 120ºC for 5 h. Nitrogen adsorption/desorption isotherms were then determined on an Autosorb-iQ automated gas-sorption analyzer (Quantachrome Instruments Inc., Boynton Beach, Florida, USA).

Cu(II) adsorption

A Cu(II) solution was prepared by dissolving an appropriate quantity of $CuSO_4{\cdot}5H_2O$ in DDW. Batch adsorption experiments were conducted in 100 mL polypropylene centrifuge tubes by adding approximately 0.05 g of RL-LDH in 50 mL of a Cu(II) solution of the required concentration. The suspensions were agitated by shaking at 160 rpm in a reciprocal water-bath shaker to achieve adsorption equilibrium. Then, the suspensions were centrifuged at 13,350×g for 30 min. The Cu(II)

https://doi.org/10.1346/CCMN.2016.064034 Published online by Cambridge University Press

concentration in the supernatant was measured using a Z-2000 flame atomic absorption spectrometer (Hitachi Ltd., Tokyo, Japan). Centrifuge tube wall adsorption was determined by shaking Cu(II) solution in centrifuge tubes without adsorbents, which indicated no adsorption to centrifuge tubes. The batch experiments were performed in triplicate, the results were reproducible within ±5%, and the average values were reported.

The effect of contact time was examined by equilibrating several sets of 100 mg L^{-1} Cu(II) solutions with 0.05 g of RL-LDH for 0−300 min. The effect of Cu(II) concentrations on adsorption was evaluated by adding 0.05 g of RL-LDH to 50 mL of 5−100 mg L^{-1} Cu(II) solutions. The amounts adsorbed were calculated after adsorption equilibrium. The effect of 5.0−10.0 initial solution pHs on Cu(II) adsorption was examined. The pHs of 100 mg L^{-1} Cu(II) solutions were adjusted by adding small amounts of 0.1 mol L^{-1} HCl or NaOH solutions. The initial pHs and final pHs after adsorption equilibrium were measured using a pHS-3C digital pH-meter (Leici Company, Shanghai, China). The effect of temperature on the adsorption characteristics of RL-LDH for Cu(II) was investigated by determining adsorption isotherms at 293 K, 303 K, and 313 K. Background electrolytes used in ionic strength studies were 0.01 and 0.10 mol L^{-1} NaCl. For comparison, the effects of contact time, Cu(II) concentration, and initial solution pH on Cu(II) adsorption to LDH were investigated. The adsorption of Cu(II) was measured without added electrolytes at pH 5.5 and 293 K, except where noted.

RESULTS AND DISCUSSION

Structure analysis

The PXRD patterns of the pristine LDH (Figure 1a) exhibited all the characteristic diffraction peaks of hydrotalcite and showed a *d* spacing of 0.90 nm, which was similar to that reported in the literature (Wu *et al*., 2005). Accordingly, the LDH exhibited a gallery height of 0.42 nm due to a brucite-like layer thickness of 0.48 nm (Wang *et al*., 2010). A schematic structural diagram of LDH is shown in Figure 2. The PXRD pattern of RL-LDH (Figure 1a) exhibited characteristic diffraction peaks of hydrotalcite with a distinct peak at 3.39 nm. This result suggests that RL^- anions can be reassembled into LDH interlayers and increase the interlayer *d* spacing of LDH. The gallery height of the RL-LDH composite was approximately 2.91 (= 3.39−0.48) nm. Based on the end-to-end RL^- anion length of 1.77 nm (Bai *et al*., 1997) and the arrangement of RL^- anions in the gallery, a possible orientation of RL^- anions was proposed (Figure 2). The RL^- anions can arrange to interpenetrate LDH interlayers as a slightly tilted bilayer, in which carboxylate groups interact with the LDH layer surface.

The FTIR spectra of LDH and RL-LDH (Figure 1b) revealed that both LDH and RL-LDH showed the characteristic IR absorption peaks of LDH (Chuang *et al*., 2010). Additionally, RL-LDH showed: (1) ~2930 and 2855 cm^{-1} bands due to the -CH_2 stretching vibration; (2) ~1565 and 1407 cm^{-1} bands associated with the carboxyl stretching vibrations of $-COO^-$ and −COOH groups, which indicate the −COOH group was also in the RL-LDH gallery. The NO_3^- ion vibration mode at ~1390 cm^{-1} in RL-LDH disappeared after the reassembly of LDH with RL^- and indicates NO_3^- anion replacement by RL anions through the delamination/reassembling process.

The TG-DSC curves of LDH and RL-LDH samples (Figure 1c) showed a weight loss of about 7.58% between 150ºC and 210ºC and an exothermic peak at ~180ºC were mainly induced by decomposition of RL^- anions. The sharp exothermic peaks at approximately 321.0ºC corresponded to the complete decomposition of the species derived from the RL^- anions.

The SEM (Figure 1d) and TEM images (Figure 1e) of LDH and RL-LDH samples showed that LDH particles were mainly hexagonal platelets with sizes between 50 nm and 100 nm: however, the RL-LDH particles were aggregated, which was induced by the introduction of RL^- anions. The plate-shaped morphology remained visible after the intercalation of RL^- anions and RL-LDH particle surfaces were smooth (Figure 1d).

The C, H, and N contents and Mg/Al molar ratios for LDH and RL-LDH are summarized in Table 1. The Mg/Al molar ratios in LDH and RL-LDH approximated the theoretical value. However, several CO_3^{2-} anions were identified in the LDH despite the use of CO_2-free DDW in the experiments. This finding could be attributed to the high affinity between CO_3^{2-} and LDH (Miyata 1983). As a result, after the reassembly of LDH with RL^- anions, the C and H contents increased, whereas the N content decreased. This phenomenon indicated that NO_3^- anions in the pristine LDH interlayers can be replaced by RL^- anions.

The specific surface area affects the adsorption performance of an adsorbent. Adsorption performance can be improved by using adsorbents with a large specific surface area. The specific surface areas of LDH and RL-LDH (Table 1) were 39.39 and 11.71 $m^2\ g^{-1}$, respectively. The surface area decrease could be due to the aggregation of RL-LDH plates (Figure 1e) and the stacking of RL^- anions in the interlayer spaces of LDH. A similar phenomenon was reported in an LDH modified with dodecylsulfate anions (Ruan *et al*., 2013).

Effect of initial solution pH on Cu(II) removal

Solution pH influences Cu(II) removal at the solid-liquid interface, metal dissolution from LDH (or RL-LDH), and Cu speciation. As such, experiments using pHs that ranged from 5.0 to 10.0 were conducted at 293 K to determine the influence of initial solution pH on Cu(II) removal. Additionally, the initial solution pH, the final pH after adsorption, and the amount of Cu(II)

https://doi.org/10.1346/CCMN.2016.064034 Published online by Cambridge University Press

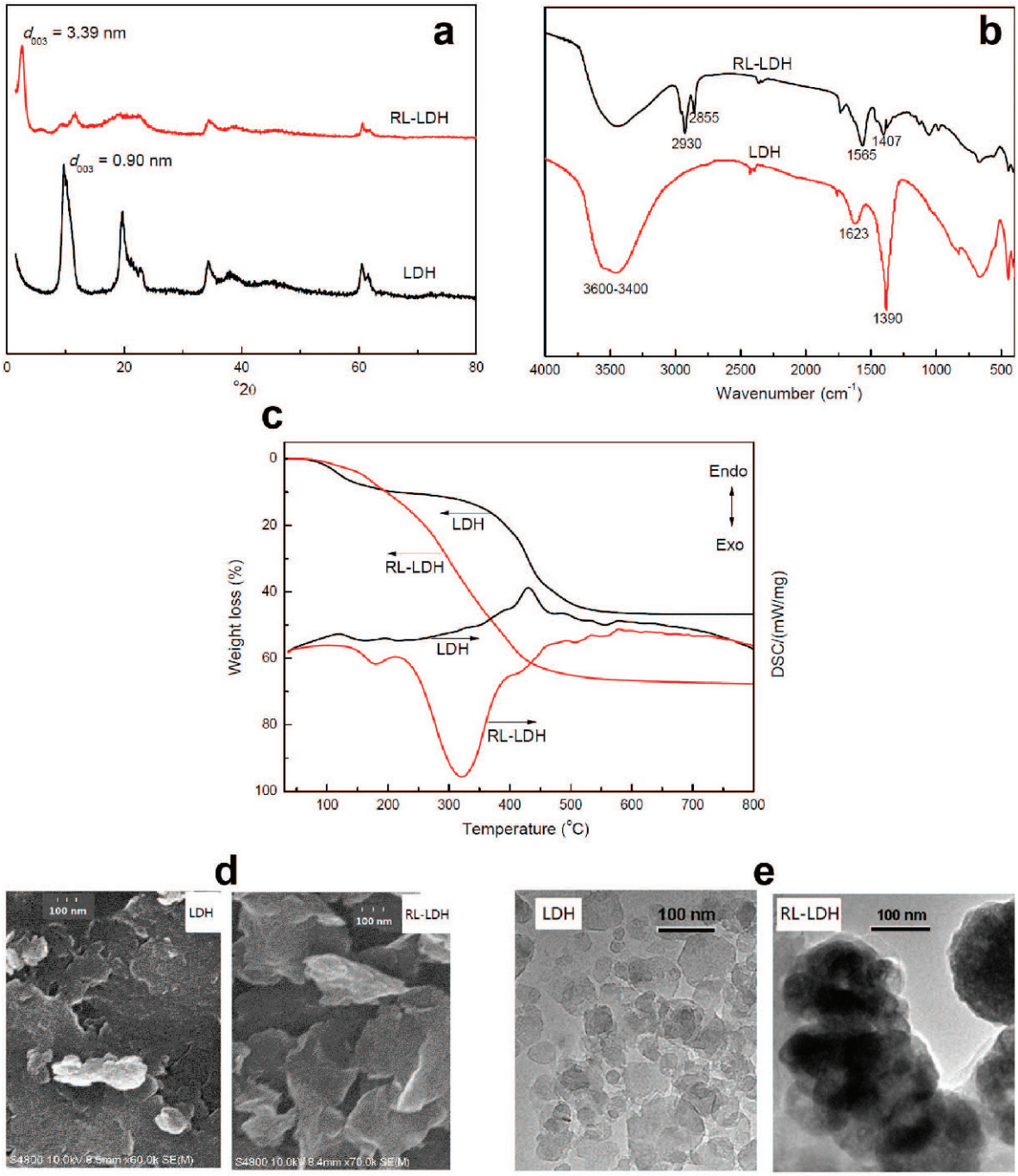

Figure 1. PXRD patterns (a), FTIR spectra (b), TG-DSC curves (c), scanning electron micrographs (d), and LDH and RL-LDH transmission electron micrographs (e).

removed at different pHs were determined (Table 2). An increase in pH dramatically increased the amount of Cu(II) removed by LDH, but only slightly increased Cu(II) removal by RL-LDH. In aqueous solutions, Cu(II) can exist as Cu^{2+}, $Cu(OH)^{+}$, $Cu(OH)_2$, $[Cu(OH)_3]^{-}$, or $[Cu(OH)_4]^{2-}$, and Cu^{2+} is the predominant species at pH < 6.0, whereas insoluble $Cu(OH)_2$ is the main species at pH > 6.3 (Sheng *et al*., 2010; Zhao *et al*., 2010b). In the present study, Cu(II) removal by LDH was rapidly enhanced after reaching pHs > 6.0, which is the pH that Cu(II) hydroxide starts to precipitate. Similar observations were reported by Bosso and Enzweiler (2002) for the adsorption of Cu(II) on scolecite. Thus, the optimum pH for Cu(II) adsorption was found to be within the pH

https://doi.org/10.1346/CCMN.2016.064034 Published online by Cambridge University Press

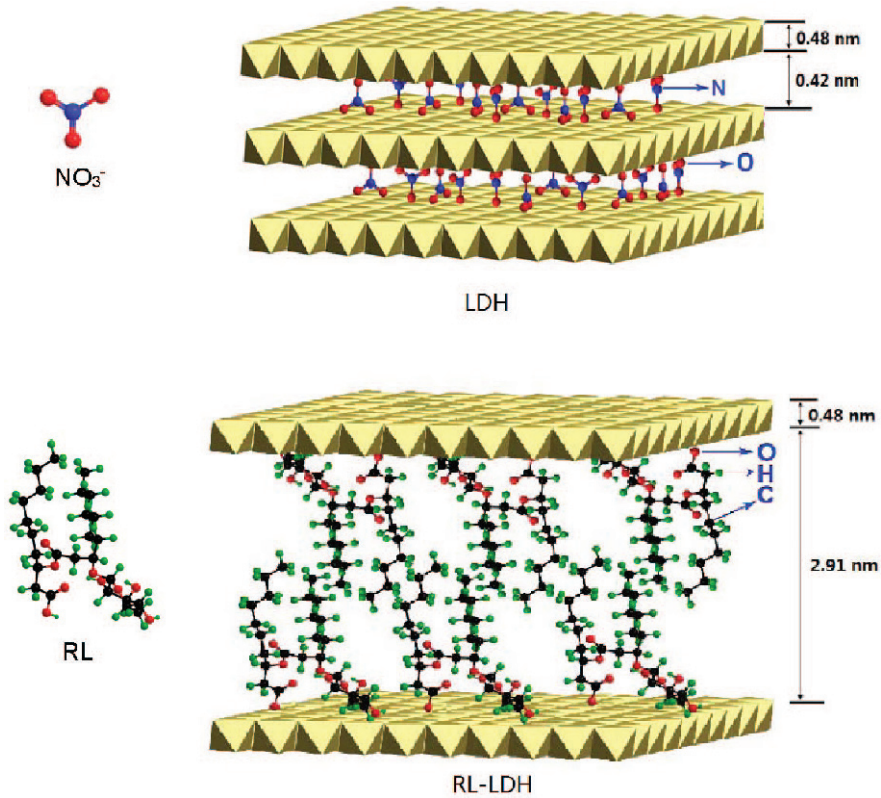

Figure 2. Schematic structural diagrams of LDH and RL-LDH.

range of 5.0−6.0 to avoid $Cu(OH)_2$ formation. At pH 5.0−6.0, the amounts of Cu(II) adsorbed to RL-LDH were higher than that to LDH. This finding suggests that RL molecules play important roles in Cu(II) adsorption. Further experiments were then conducted at pH 5.5.

Adsorption kinetics

The influence of contact time on adsorption were demonstrated. The adsorption rate of Cu(II) on LDH or RL-LDH (Figure 3) was rapid in the initial stages and gradually decreased with increasing adsorption time until reaching equilibrium. The equilibrium time for Cu(II) adsorption on LDH (and RL-LDH) was less than 250 (and 120) min; therefore, the adsorption times of 250 and 120 min were selected, respectively, in other experiments.

Kinetics models are used to elucidate the adsorption mechanism and evaluate the performance of adsorbents for Cu(II) removal. In this study, adsorption kinetics of Cu(II) adsorption to LDH and RL-LDH were evaluated by fitting the experimental data (Figure 3) using pseudo-first-order and pseudo-second-order kinetics models (Table 3). First, adsorption kinetics were analyzed using the following pseudo-first-order equation given by Lagergren (1898).

$$\ln(q_e - q_t) = \ln q_e - k_1 t \quad (1)$$

where q_e and q_t (mg g^{-1}) are the amounts of Cu(II) adsorbed at equilibrium and at time t (min), respectively, and k_1 (min^{-1}) is the rate constant.

Experimental data were then modeled according to pseudo-second-order kinetics, given in the following form (Gosset *et al.*, 1986):

$$\frac{t}{q_t} = \frac{1}{k_2 q_e^2} + \frac{t}{q_e} \quad (2)$$

Table 1. Properties of synthesized LDH and RL-LDH samples.

Material	Mg^{2+}/Al^{3+} (molar ratio)	N (wt.%)	C (wt.%)	H (wt/%)	Specific surface area (m^2 g^{-1})
LDH	2.96	3.60	0.29	3.65	39.39
RL-LDH	2.81	0.18	37.22	7.47	11.71

https://doi.org/10.1346/CCMN.2016.064034 Published online by Cambridge University Press

Table 2. Influence of initial pH on Cu(II) removed by LDH and RL-LDH (adsorption conditions: 293 K, 2 g L^{-1} LDH or RL-LDH, cCu(II) = 100 mg L^{-1}).

Adsorbent (g L^{-1})	Time (min)	Initial pH	Final pH	Removal amount (mg g^{-1})
LDH	250	5.05	5.84	5.87
		6.01	6.78	19.85
		7.21	7.67	50.79
		8.17	7.51	58.62
		9.06	9.09	59.16
		10.08	10.07	59.17
RL-LDH	120	5.05	5.49	54.12
		6.01	6.42	55.62
		7.21	7.38	57.87
		8.17	8.29	58.62
		9.06	9.08	59.15
		10.08	10.09	59.18

where q_e and q_t are defined similar to those in equation 1, and k_2 (g mg^{-1} min^{-1}) is the rate constant.

The correlation coefficient (R^2) values (Table 3) showed that the kinetics data for Cu(II) adsorption on LDH and RL-LDH were optimally described by the pseudo-first-order and pseudo-second-order kinetics models, respectively. Moreover, the experimental equilibrium adsorption capacities ($q_{e,exp}$) determined from the study on contact time were in agreement with the theoretical equilibrium adsorption capacities ($q_{e,cal}$) calculated using the corresponding kinetics model. The Cu(II) adsorption kinetics of LDH fitted the pseudo-first-order kinetics model well and implies that a reversible reaction was established between the liquid and solid phases at equilibrium. Furthermore, because the Cu(II) adsorption kinetics to RL-LDH followed the pseudo-second-order model, the adsorption mechanism (*i.e.*, chemical binding, not mass transport) of chemical binding was the rate-limiting step of the adsorption process (Sağ *et al.*, 2001). The results were in accord with the relatively low specific surface areas of RL-LDH (Table 1). The adsorption of functional groups might primarily determine the adsorption process, indicating that adsorption to the nanocomposite is similar to a chemisorption process.

Investigation of equilibrium adsorption isotherms

The effect of initial Cu(II) concentrations (5−100 mg L^{-1}) on Cu(II) adsorption to LDH and RL-LDH (Figure 4) showed that RL-LDH adsorbed higher amounts of Cu(II) than LDH at any equilibrium Cu(II) concentration at 293 K. Initial Cu(II) concentration was an important driving force to overcome the mass transfer resistance of Cu(II) between aqueous and solid phases. As such, high initial Cu(II) concentrations

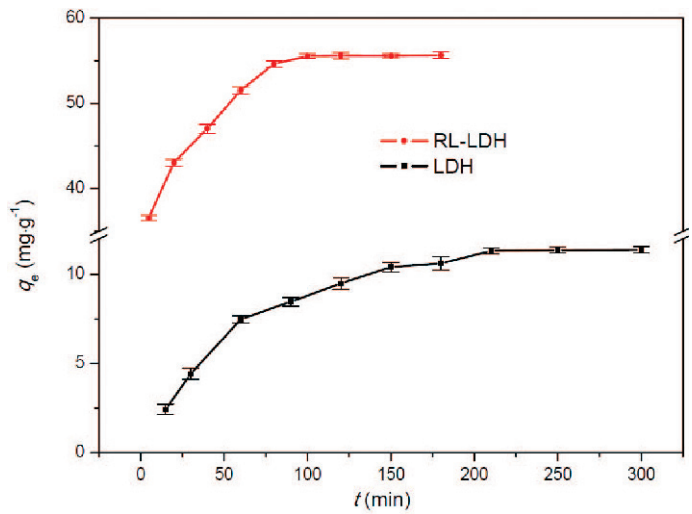

Figure 3. Influence of interaction time on Cu(II) adsorption (mg g^{-1}) by LDH and RL-LDH (adsorption conditions: 293 K, 2 g L^{-1} LDH or RL-LDH, c Cu(II) = 100 mg L^{-1}, and pH = 5.5).

https://doi.org/10.1346/CCMN.2016.064034 Published online by Cambridge University Press

Table 3. Parameters for pseudo-first-order and pseudo-second-order kinetics models for Cu(II) adsorption on LDH and RL-LDH (adsorption conditions: 293 K, 2 g L^{-1} LDH or RL-LDH, pH = 5.5, and *c*Cu(II) = 100 mg L^{-1}).

Kinetics model	Parameter	Adsorbent	
		LDH	RL-LDH
pseudo-first-order	$q_{e,exp}$ (mg g^{-1})	11.21	55.68
	k_1 (min^{-1})	0.02	0.04
	$q_{e,cal}$ (mg g^{-1})	11.26	32.93
	R^2	0.9918	0.9358
pseudo-second-order	k_2 (g mg^{-1} min^{-1})	0.0012	0.0031
	$q_{e,cal}$ (mg g^{-1})	13.87	57.14
	R^2	0.9928	0.9988

could enhance the adsorption process. Additionally, increasing the initial Cu(II) concentration could increase the probability of contact between Cu(II) and LDH (or RL-LDH).

Adsorption isotherm models were used to determine the adsorption mechanism. As such, the adsorption data (Figure 4) were analyzed using three isotherms, namely, Langmuir, Freundlich, and Dubinin-Radushkevich (D-R).

In the Langmuir isotherm, the basic assumption is that adsorption occurs at specific homogeneous sites within the adsorbent; the isotherm equation is described as follows (Langmuir, 1916):

$$\frac{c_e}{q_e} = \frac{1}{q_m} \cdot c_e + \frac{1}{K_L q_m} \quad (3)$$

where c_e (mg L^{-1}) is the equilibrium Cu(II) concentration, q_e (mg g^{-1}) is the amount adsorbed, q_m (mg g^{-1}) is the maximum monolayer adsorption capacity adsorbed on the adsorbent, and K_L (L mg^{-1}) is the Langmuir constant related to adsorption energy. A higher K_L value indicates a higher affinity.

The Freundlich isotherm is derived by assuming the presence of a heterogeneous surface with a non-uniform heat of adsorption distribution on the surface. This isotherm can be expressed as follows (Freundlich, 1906):

$$\ln q_e = \ln K_F + 1/n \ln c_e \quad (4)$$

where K_F ($L^{1/n}$ $mg^{(1-1/n)}$ g^{-1}) and n (dimensionless) are the Freundlich isotherm constant and heterogeneity factor (adsorption intensity or surface heterogeneity), respectively.

The Dubinin-Radushkevich (D-R) adsorption isotherm predicts the adsorption energy per unit of adsorbate and the maximum adsorption capacity for the adsorbent. The equation is expressed as follows (Dubinin and Radushkevich, 1947):

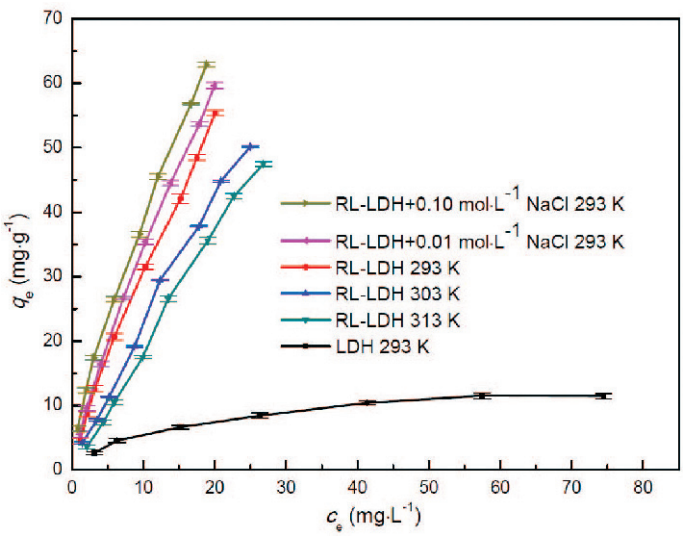

Figure 4. Influence of Cu(II) concentration and ionic strength on Cu(II) adsorption (mg g^{-1}) to LDH and RL-LDH (adsorption conditions: 2 g L^{-1} LDH or RL-LDH, pH = 5.5). For a grayscale image, the top-to-bottom order of six plots in the figure is the same as the order in the legend.

https://doi.org/10.1346/CCMN.2016.064034 Published online by Cambridge University Press

$$\ln q_e = \ln q_s - \beta\varepsilon^2 \quad (5)$$

where q_s (mg g^{-1}) is the D-R constant, and ε can be correlated to temperature as follows:

$$\varepsilon = RT \ln\left(1 + \frac{1}{c_e}\right) \quad (6)$$

The constant β provides the mean free energy E of adsorption per adsorbate molecule when a molecule is transferred from the bulk solution to the solid surface. This energy can be calculated using the following relationship:

$$E = \frac{1}{\sqrt{2\beta}} \quad (7)$$

where E (kJ mol^{-1}) describes the type of adsorption. If E < 8 kJ mol^{-1}, the adsorption proceeds through a physical mechanism, whereas if E ranges from 8 kJ mol^{-1} to 16 kJ mol^{-1}, the adsorption is controlled by a chemical mechanism (Onyango *et al*., 2006).

Langmuir, Freundlich, and D-R isotherm constants were determined from the plots of c_e/q_e *vs.* c_e, $\ln q_e$ *vs.* $\ln c_e$, and $\ln q_e$ *vs.* ε^2, respectively, at 293 K. All R^2 values (Table 4) were higher than 0.91, which indicated that Cu(II) adsorption on LDH and RL-LDH was a complex process, *i.e.*, the adsorption cannot be described by a definite adsorption isotherm model but can be described using a combination of these models. For LDH, the Langmuir isotherm showed the highest R^2 values in comparison to the Freundlich and D-R isotherms and suggests that the adsorption occurred at specific homogeneous sites within LDH. For RL-LDH, the Freundlich isotherm had the highest R^2 values in comparison to the other isotherms. The high R^2 values of the Freundlich isotherm model suggests that adsorption occurred at heterogeneous, consistent, and well distributed active sites along the RL-LDH surface. The high K_F value reflected a high adsorption capacity. Moreover, high $1/n$ values reflect the heterogeneity of the adsorbent sites. Above all, RL-LDH had a greater Cu(II) adsorption capacity than LDH. Similarly, the Langmuir isotherm data indicated that RL-LDH had a higher Cu(II) adsorption capacity and affinity than LDH. The E values obtained from the D-R isotherm equation suggested that Cu(II) adsorption on LDH and RL-LDH occurred by way of physical and chemical mechanisms, respectively.

The Cu(II) adsorption by LDH could result from the linking electrostatic effects of SO_4^{2-} anions from the $CuSO_4$ solution between the positively charged LDH surface and the Cu(II) cations (Zang *et al*., 2011). The Cu(II) adsorption capacity of RL-LDH was higher than LDH under the same conditions, which indicates that interlayer RL^- anions induced Cu(II) adsorption from the aqueous solution. In other words, the RL^- anions formed complexes with Cu(II) because the carboxylate groups served as active sites for Cu(II) adsorption, thereby increasing the adsorption capacity. With the formation of the complexes, the SO_4^{2-} anions were presumed to be intercalated in the interlayers of RL-LDH to compensate the extra positive charge from Cu^{2+}, *i.e.*, the SO_4^{2-} anions were also intercalated in RL-LDH interlayers along with the adsorbed Cu^{2+}. A similar result was reported for the adsorption of Cu^{2+} on a Mg-Al layered double hydroxide intercalated with ethylenediaminetetraacetate anion by Kameda (2005).

Effect of temperature on adsorption and thermodynamic study

The effect of temperature on Cu(II) adsorption by RL-LDH (Figure 4) was investigated within different temperature ranges (293−313 K) at pH 5.5 and at a contact time of 120 min. The amount of adsorbed Cu(II) decreased with increased temperature, which indicated the exothermic nature of the adsorption process.

Table 4. Adsorption isotherm parameters for Cu(II) adsorption on LDH and RL-LDH (adsorption conditions: 293 K, 2 g L^{-1} LDH or RL-LDH, and pH = 5.5).

Adsorbents *Langmuir*	K_L (L mg^{-1})	q_m (mg g^{-1})	R^2
LDH	0.08	13.18	0.9978
RL-LDH	0.03	140.45	0.9343
Freundlich	K_F ($L^{1/n}$ $mg^{(1-1/n)}$ g^{-1})	$1/n$	R^2
LDH	1.81	0.45	0.9469
RL-LDH	4.53	0.83	0.9981
D-R	q_s (mg g^{-1})	E (kJ mol^{-1})	R^2
LDH	36.43	7.45	0.9909
RL-LDH	260.16	8.45	0.9791

https://doi.org/10.1346/CCMN.2016.064034 Published online by Cambridge University Press

Table 5. Gibbs free energy, enthalpy, and entropy changes associated with Cu(II) adsorption on RL-LDH (adsorption conditions: 2 g L^{-1} LDH or RL-LDH, and pH = 5.5).

T (K)	ΔG (kJ mol^{-1})	ΔH (kJ mol^{-1})	ΔS (mol^{-1} K^{-1})
293	−3.74	−42.17	−131.16
303	−2.43		
313	−1.11		

Thermodynamic parameters, namely, Gibbs free energy (Δ*G*), enthalpy (Δ*H*), and entropy (Δ*S*) changes, were calculated using the following equations (Zhao *et al*., 2010a):

$$\ln K_d = -\frac{\Delta H}{RT} + \frac{\Delta S}{R} \quad (8)$$

$$K_d = \frac{q_e}{c_e} \quad (9)$$

$$\Delta G = -RT\ln K_d = \Delta H - T\Delta S \quad (10)$$

where *T* is temperature (K), K_d is the distribution coefficient (L g^{-1}), and R is the standard molar gas constant (8.314 J mol^{-1} K^{-1}). The Δ*H* and Δ*S* values were obtained from the slope and intercept of plots ($\ln K_d$ *vs.* 1/*T*). The Δ*G* value was calculated by equation 10 at different temperatures.

The values of the thermodynamic parameters obtained from the fitted line (Table 5) showed that: (1) the absolute value of Δ*H* was higher than 42 kJ mol^{-1}, which suggests that adsorption was a chemisorption process (Hatay *et al*., 2008; Zhang, *et al*., 2014); (2) the values of Δ*G* and Δ*H* were all negative, which indicates the adsorption was spontaneous and exothermic, *i.e.*, the coordination of RL^- anions and Cu(II) cations can spontaneously drive the Cu(II) into RL-LDH interlayers; (3) the value of Δ*G* decreased with the decreased temperature, which means lower temperatures favored the adsorption process; and (4) after Cu(II) adsorption, entropy was reduced and randomness decreased.

Effect of ionic strength on adsorption

Various kinds of ions exist in wastewater and the electrolyte concentration can affect adsorbate-adsorbent interactions (Anirudhan *et al*., 2009); therefore, the influence of ionic strength on Cu(II) adsorption was investigated. The amount of Cu(II) adsorbed increased when NaCl concentrations were increased from 0.00 to 0.01 and 0.10 mol L^{-1} (Figure 4). Based on the FTIR characterization, −COOH groups on RL molecules were also intercalated in LDH interlayers. When NaCl was added to the adsorption suspension at pH 5.5, the dissociation of −COOH into $-COO^-$ increased due to the salt effect, so more RL^- ($-COO^-$) anions could complex with Cu(II) to increase the amount of Cu(II) adsorbed.

Comparison with other adsorbents

The data for Cu(II) adsorption by RL-LDH (Table 4) had a Langmuir isotherm R^2 of 0.9343, which indicates a comparatively good fit. The maximum adsorption capacity (q_m) obtained using a fit of the data to the Langmuir isotherm was compared to the maximum adsorption capacities of other clay adsorbents previously studied (Table 6). The Cu(II) adsorption capacity of the RL-LDH at 293 K was 140.45 mg g^{-1}, which was higher than that of LDH (13.18 mg g^{-1}). Furthermore, the Cu(II) adsorption capacity of RL-LDH was higher than an acid-activated montmorillonite (Bhattacharyya *et al*., 2011), a sulfonated lignin-LDH composite (Huang *et al*., 2015), an acid activated bentonite (Koyuncu *et al*., 2014), and a chitosan-zeolite composite (Wan Ngah *et al*., 2013). Differences in the Cu(II) adsorption capacity could be due to the distinct properties of each adsorbent, particularly in terms of structure, functional groups, and surface area. The results of the comparison confirm that RL-LDH can be used for Cu(II) removal.

CONCLUSIONS

A novel adsorbent, RL-LDH, was synthesized by a delamination/reassembling process and used to remove Cu(II) from aqueous solutions. The fit of the Cu(II) adsorption to RL-LDH data using the pseudo-second-order kinetics model was good and was more accurately described using the Freundlich isotherm model than the Langmuir or D-R isotherm models. The Cu(II) adsorption capacity of RL-LDH depended on initial solution pH, temperature, initial concentration, and ionic strength and could be mainly attributed to the formation of an

Table 6. Maximum Cu(II) adsorption capacities for various adsorbents.

Adsorbent	*T* (K)	q_m (mg g^{-1})	Reference
Acid-activated montmorillonite	303	32.30	Bhattacharyya *et al*., 2011
Sulfonated lignin-LDH	Room *T*.	71.40	Huang *et al*., 2015
Acid activated bentonite	303	38.31	Koyuncu *et al*., 2014
Chitosan-zeolite composite	298	51.32	Wan Ngah *et al*., 2013
LDH	293	13.18	This study
RL-LDH	293	140.15	This study

https://doi.org/10.1346/CCMN.2016.064034 Published online by Cambridge University Press

interlayer RL-Cu(II) complex in RL-LDH. The adsorption of Cu(II) was found to be a spontaneous and exothermic chemisorption process. This study revealed that RL-LDH can be an efficient potential adsorbent because of its outstanding performance in Cu(II) removal from wastewater, and a magnetite Fe_3O_4@(RL-LDH) nanocomposite is expected to be a useful material to effectively remove Cu(II) in wastewater treatment.

ACKNOWLEDGMENTS

This work was supported by the Natural Science Foundation of Shanxi Province of China (2013011040-8), National Training Programs of Innovation and Entrepreneurship for Undergraduates (201310122002), and Training Programs of Innovation and Entrepreneurship for Undergraduates in Shanxi (2014431).

REFERENCES

Anirudhan, T.S., Jalajamony, S., and Suchithra, P.S. (2009) Improved performance of a cellulose-based anion exchanger with tertiary amine functionality for the adsorption of chromium (VI) from aqueous solutions. *Colloids and Surfaces A-Physicochemical and Engineering Aspects*, **335**, 107–113.

Awual, M.R., Ismael, M., Yaita, T., El-Safty, S.A., Hideaki, S., Okamoto, Y., and Suzuki, S. (2013) Trace copper(II) ions detection and removal from water using novel ligand modified composite adsorbent. *Chemical Engineering Journal*, **222**, 67–76.

Bai, G., Brusseau, M.L., and Miller, R.M. (1997) Biosurfactant-enhanced removal of residual hydrocarbon from soil. *Applied and Environmental Microbiology*, **63**, 157–170.

Bhattacharyya, K.G. and Gupta, S.S. (2011) Removal of Cu(II) by natural and acid-activated clays: An insight of adsorption isotherm, kinetic and thermodynamics. *Desalination*, **272**, 66–75.

Bosso, S.T. and Enzweiler, J. (2002) Evaluation of heavy metal removal from aqueous solution onto scolecite. *Water Research*, **36**, 4795–4800.

Chuang, Y.H., Liu, C.H., Tzou, Y.M., Chang, J.S., Chiang, P.N., and Wang, M.K. (2010) Comparison and characterization of chemical surfactants and bio-surfactants intercalated with layered double hydroxides (LDHs) for removing naphthalene from contaminated aqueous solutions. *Colloids and Surfaces A-Physicochemical and Engineering Aspects*, **366**, 170–177.

da Fonseca, M.G., de Oliveira, M.M., Arakaki, L.N.H., Espinola, J.G.P., and Airoldi, C. (2005) Natural vermiculite as an exchanger support for heavy cations in aqueous solution. *Journal of Colloid and Interface Science*, **285**, 50–55.

Dahrazma, B. and Mulligan, C.N. (2007) Investigation of the removal of heavy metals from sediments using rhamnolipid in a continuous flow configuration. *Chemosphere*, **69**, 705–711.

Dubinin, M.M. and Radushkevich, L.V. (1947) Equation of the characteristic curve of activated charcoal. *Proceedings of the Academy of Sciences of the USSR, Physical Chemistry Section*, **55**, 331–333.

Freundlich, H.M.F. (1906) Over the adsorption in solution. *Journal of Physical Chemistry*, **57**, 385–470.

Gosset, T., Trancart, J.L., and Thevenot, D.R. (1986) Batch metal removal by peat kinetics and thermodynamics. *Water Research*, **20**, 21–26.

Hatay, I., Gup, R., and Ersz, M. (2008) Silica gel functionalized with 4-phenylacetophynone 4-aminobenzoylhydrazone: synthesis of a new chelating matrix and its application as metal ion collector. *Journal of Hazardous Materials*, **150**, 546–553.

Huang, G., Wang, D., Ma, S., Chen, J., Jiang, L., and Wang, P. (2015) A new, low-cost adsorbent: Preparation, characterization, and adsorption behavior of Pb(II) and Cu(II). *Journal of Colloid and Interface Science*, **445**, 294–302.

Inyang, M., Gao, B., Yao, Y., Xue, Y., Zimmerman, A.R., Pullammanappallil, P., and Cao, X. (2012) Removal of heavy metals from aqueous solution by biochars derived from anaerobically digested biomass. *Bioresource Technology*, **110**, 50–56.

Kameda, T., Saito, S., and Umetsu Y. (2005) Mg-Al layered double hydroxide intercalated with ethylene-diaminetetraacetate anion: Synthesis and application to the uptake of heavy metal ions from an aqueous solution. *Separation and Purification Technology*, **47**, 20–26.

Koyuncu, H. and Kul, A.R. (2014) An investigation of Cu(II) adsorption by native and activated bentonite: Kinetic, equilibrium and thermodynamic study. *Journal of Environmental Chemical Engineering*, **2**, 1722–1730.

Lagergren, S. (1898) Zur theorie der sogenannten adsorption gelöster stoffe. *Kungliga Svenska Vetenskapsakademiens. Handlingar*, **24**, 1–39.

Langmuir, I. (1916) The constitution and fundamental properties of solids and liquids. Part I. Solids. *Journal of the American Chemical Society*, **38**, 2221-2295,

Lu, X., Meng, L., Li, H., Du, N., Zhang, R., and Hou, W. (2013) Facile fabrication of ibuprofen-LDH nanohybrids via a delamination/reassembling process. *Materials Research Bulletin*, **48**, 1512–1517.

Matlock, M.M., Howerton, B.S., and Atwood, D.A. (2002) Chemical precipitation of heavy metals from acid mine drainage. *Water Research*, **36**, 4757–4764.

Miyata, S. (1983) Anion-exchange properties of hydrotalcite-like compounds. *Clays and Clay Minerals*, **31**, 305–311.

Mohammadi, T., Moheb, A., Sadrzadeh, M., and Razmi, A. (2005) Modeling of metal ion removal from wastewater by electrodialysis. *Separation and Purification Technology*, **41**, 73–82.

Mulligan, C.N. (2009) Recent advances in the environmental applications of biosurfactants. *Current Opinion in Colloid and Interface Science*, **14**, 372–378.

Ochoa-Loza, F.J., Artiola, J.F., and Maier, R.M. (2001) Stability constants for the complexation of various metals with a rhamnolipid biosurfactant. *Journal of Environmental Quality*, **30**, 479–485.

Onyango, M.S., Kojima,Y., Kumar, A., and Kuchar, D. (2006) Uptake of fluoride by Al^{3+} pretreated low-silica synthetic zeolites: adsorption equilibrium and rate studies. *Separation and Purification Technology*, **41**, 683–704.

Qiu, D. and Hou, W. (2009) Synthesis and characterization of indole-3-butyric acid/hydrotalcite-like compound nanohybrids. *Colloids and Surfaces A-Physicochemical and Engineering Aspects*, **336**, 12–17.

Ruan, X., Huang, S., Chen, H., and Qian, G. (2013) Sorption of aqueous organic contaminants onto dodecyl sulfate intercalated magnesium iron layered double hydroxide. *Applied Clay Science*, **72**, 96–103.

Sağ, Y. and Aktay, Y. (2001) Mass transfer and equilibrium studies for the sorption of chromium ions onto chitin. *Process Biochemistry*, **36**, 157–173.

Shan, R.R., Yan, L.G., Yang, K., Yu, S.J., Hao, Y.F., Yu, H.Q., and Du B. (2014) Magnetic Fe_3O_4/MgAl-LDH composite for effective removal of three red dyes from aqueous solution. *Chemical Engineering Journal*, **252**, 38–46.

Sheng, G.D., Li, J.X., Shao, D.D., Hu, J., Chen, C.L., Chen, Y.X., and Wang, X.K. (2010) Adsorption of copper(II) on multiwalled carbon nanotubes in the absence and presence of humic or fulvic acids. *Journal of Hazardous Materials*, **178**, 333–340.

Sud, D., Mahajan, G., and Kaur, M.P. (2008) Agricultural waste material as potential adsorbent for sequestering heavy metal ions from aqueous solutions – a review. *Bioresource Technology*, **99**, 6017–6027.

Torrens, J.L., Herman, D.C., and Maier, R.M. (1998) Biosurfactant (rhamnolipid) sorption and the impact on rhamnolipid-facilitated removal of cadmium from various soils under saturated flow conditions. *Environmental Science & Technology*, **32**, 776–781.

Venkateswaran, P., Gopalakrishnan, A.N., and Palanivelu, K. (2007) Di(2-ethylhexyl)phosphoric acid-coconut oil supported liquid membrane for the separation of copper ions from copper plating wastewater. *Journal of Environmental Sciences*, **19**, 1446–1453.

Wan Ngah, W.S., Teong, L.C., Toh, R.H., and Hanafiah, M.A.K.M. (2013) Comparative study on adsorption and desorption of Cu(II) ions by three types of chitosan-zeolite composites. *Chemical Engineering Journal*, **223**, 231–238.

Wang, J., Zhou, J., Li, Z., Song, Y., Liu, Q., Jiang, Z., and Zhang, M. (2010) Magnetic, luminescent Eu-doped Mg-Al layered double hydroxide and its intercalation for ibuprofen. *Chemistry – A European Journal*, **16**, 14404–14411.

Wu, Q., Olafsen, A., Vistad, Ø.B., Roots, J., and Norby, P. (2005) Delamination and restacking of a layered double hydroxide with nitrate as counter anion. *Journal of Materials Chemistry*, **15**, 4695–4700.

Zang, Y.B., Hou, W.G., and Xu, J. (2011) Removal of Cu(II) from $CuSO_4$ aqueous solution by Mg-Al hydrotalcite-like compounds. *Chinese Journal of Chemistry*, **29**, 847–852.

Zhang, Y., Chen, Y., Wang, C., and Wei, Y. (2014) Immobilization of 5-aminopyridine-2-tetrazole on cross-linked polystyrene for the preparation of a new adsorbent to remove heavy metal ions from aqueous solution. *Journal of Hazardous Materials*, **276**, 129–137.

Zhao, Y.G., Shen, H.Y., Pan, S.D., Hu, M.Q., and Xia, Q.H. (2010a) Preparation and characterization of amino-functionalized nano-Fe_3O_4 magnetic polymer adsorbents for removal of chromium(VI) ions. *Journal of Materials Science*, **45**, 5291–5301.

Zhao, G., Zhang, H., Fan, Q., Ren, X., Li, J., Chen, Y., and Wang, X. (2010b) Sorption of copper(II) onto super-adsorbent of bentonite-polyacrylamide composites. *Journal of Hazardous Materials*, **173**, 661–668.

(*Received 28 February 2016; revised 15 September 2016; Ms. 1092; AE: A. Neumann*)